THE JOURNAL OF PHYSICAL CHEMISTRY B

Article

pubs.acs.org/JPCB

Temperature-Dependent Solubility Transition of Na_2SO_4 in Water and the Effect of NaCl Therein: Solution Structures and Salt Water Dynamics

Pankaj Bharmoria,[†] Praveen Singh Gehlot,[†] Hariom Gupta,[§,∥] and Arvind Kumar*[,†,‡,∥]

[†]Academy of Scientific and Innovative Research (AcSIR) and [‡]Salt and Marine Chemical Discipline, [§]Analytical Discipline & Centralized Instrument Facility, [∥]Central Salt and Marine Chemicals Research Institute, Council of Scientific & Industrial Research (CSIR), G. B. Marg, Bhavnagar-364002, Gujarat, India

Supporting Information

ABSTRACT: Dual, aqueous solubility behavior of Na_2SO_4 as a function of temperatures is still a natural enigma lying unresolved in the literature. The solubility of Na_2SO_4 increases up to 32.38 °C and decreases slightly thereafter at higher temperatures. We have thrown light on this phenomenon by analyzing the Na_2SO_4−water clusters (growth and stability) detected from temperature-dependent dynamic light scattering experiments, solution compressibility changes derived from the density and speed of sound measurements, and water structural changes/Na_2SO_4 (ion pair)−water interactions observed from the FT-IR and 2D DOSY ^{1}H NMR spectroscopic investigations. It has been observed that Na_2SO_4−water clusters grow with an increase in Na_2SO_4 concentration (until the solubility transition temperature) and then start decreasing afterward. An unusual decrease in cluster size and solution compressibility has been observed with the rise in temperature for the Na_2SO_4 saturated solutions below the solubility transition temperature, whereas an inverse pattern is followed thereafter. DOSY experiments have indicated different types of water cluster species in saturated solutions at different temperatures with varying self-diffusion coefficients. The effect of NaCl (5−15 wt %) on the solubility behavior of Na_2SO_4 at different temperatures has also been examined. The studies are important from both fundamental and industrial application points of view, for example, toward the clean separation of NaCl and Na_2SO_4 from the effluent streams of textile and tannery industries.

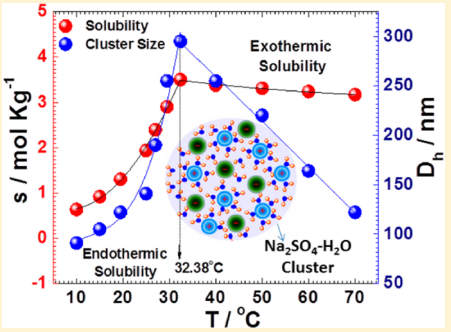

1. INTRODUCTION

Sodium sulfate (Na_2SO_4) is a mineral of universal distribution and is widely used in many chemical industries such as in detergents, pulp/paper, textiles, leather tanning, or glass and is also used as a phase change thermal energy storage material. In Na_2SO_4−H_2O systems, it occurs in two stable phases, that is, below 32.38 °C as mirabilite (Na_2SO_4·10H_2O; Glauber's salt) and above this temperature as thenardite (Na_2SO_4).[1−3] The solubility of sodium sulfate is of geological interest in connection with the natural occurrence of the minerals and water that contain it and also in reference to methods of separation and extraction from the mixtures in which it occurs. Temperature-dependent solubility behavior of Na_2SO_4, however, is peculiar among all of the alkali metals sulfates. The solubility of Li_2SO_4 decreases, and that of K_2SO_4, Rb_2SO_4, and Cs_2SO_4 increases almost linearly with the increase in temperature; a sharp increase in the solubility is observed for Na_2SO_4 up to 32.38 °C, and thereafter, it starts decreasing slightly with the further rise in temperature (Figure S1, Supporting Information).[3] Although, the release of crystal water above 32.38 °C has been cited as the reason for this behavior in the literature, surprisingly, no information is available on why such a transition occurs and how Na_2SO_4 interacts with water-saturated solutions at various temperatures. Herein, our intention is to shed light on this intriguing phenomenon that is of considerable interest both fundamentally and technically by analyzing the Na_2SO_4−water solution structures.

There are reports in the literature on the characteristics of aqueous salt solutions and their structures (existence of free ions, solvated ions, ion pairs, and higher-order clusters) investigated by employing various techniques, namely, scattering, thermodynamic, and spectroscopic.[4−22] Georgalis et al. have detected the presence of large clusters in unsaturated aqueous salt solutions under ambient conditions from dynamic light scattering (DLS) experiments.[4] In a recent paper, we have also observed very large size salt water clusters in the saturated solutions of NaCl, KCl, and NH_4Cl solutions and correlated the size and stability of clusters with their temperature-dependent solubility behavior.[5] In the saturated Na_2SO_4−water solutions, we have observed large size clusters that behaved in a peculiar fashion as a function of temperature. At the macroscopic level, thermodynamic and transport properties of aqueous salt solutions have been found useful for elucidating effect of salts on water structure and hydration of ions/ion

Received: August 6, 2014
Revised: October 14, 2014
Published: October 14, 2014

pairs.[6−12] The derived properties from the primary thermodynamic data of solutions, such as isentropic compressibility, are particularly helpful for interpreting the structural changes of water as a consequence of addition of electrolytes.[5,13−16] Herein, we have found that the compressibility changes of saturated Na_2SO_4−water solutions closely follow the Na_2SO_4−water cluster behavior detected from DLS, and the results are complementary to each other.

Salt water dynamics, particularly in concentrated solutions, are highly complex because of the existence of many species ranging from small hydrated ions/ion pairs to large salt water clusters and bulk water. Ionic charge densities govern water−ion interactions and define the relative importance of ion−water dipole interactions and the extent of hydrogen bonding between water molecules. Due to enhanced electrostatic ordering, ions with higher charge density perturb the bulk hydrogen bonding to a greater extent than larger ions with lower charge density. Through FT-IR[17−30] and NMR,[17−21,31−38] which are sensitive and noninvasive techniques, it is possible to detect the changes in the hydrogen bonding environment of water and also the shifts in ion nuclei. The water structural changes and shifts in ion nuclei are more pronounced with larger and more polarizable anions and smaller and high charge density cations such as sulfate and sodium in the present case. Because water is a highly structured liquid with distinct local structures,[39,40] the variation in temperature also has a significant effect on local structures, which can be explicitly involved in solubility limits of different salts. We have, therefore, recorded temperature-dependent FT-IR and 2D diffusion-ordered spectroscopy (DOSY) ^{1}H NMR spectra precisely to complement the DLS and compressibility information in elucidating the water structure, cluster stability, and ion pair−water interactions in the saturated Na_2SO_4 solutions. The combination of DLS and compressibility data, together with temperature-dependent FT-IR and NMR results, have enabled us to account for the solubility transition of Na_2SO_4 at 32.38 °C, unlike other alkali metal sulfates.

2. EXPERIMENTAL SECTION

2.1. Materials and Methods. NaCl and Na_2SO_4 (>99.5% by mol) were obtained from S.D. Fine Chemicals (Mumbai). Salts were used after drying in an oven at 70 °C without further purification. Aqueous Na_2SO_4 solutions were prepared by weight, using an analytical balance with a precision of ±0.0001 g (Denver Instrument APX-200) in Millipore grade water. The solubility of Na_2SO_4 in water and in aqueous NaCl solutions (5, 10, and 15 wt % NaCl) in the temperature range of 10−70 °C was determined by gravimetric and volumetric methods. Detailed procedures are provided in Annexure 1 (Supporting Information).

2.2. DLS. Cluster size measurements were performed from 10 to 70 °C using a Zetasizer Nano ZS light scattering apparatus (Malvern Instruments, U.K.) with a He−Ne laser (633 nm, 4 Mw) at a scattering angle of 90°. Salt solutions were filtered directly into quartz cell using a membrane filter of 0.45 μm pore size. The measurements were done by considering the viscosity and refractive index values (Table S1 and S3, Supporting Information) of the saturated solutions at the concerned temperature. The viscosity of solutions was measured by using Brookfield DV-II+ Pro viscometer. Refractive index measurements were done on a Mettler-Toledo (Model RE-40 D) refractometer having a high-resolution optical sensor. Measurements were made with a resolution and limit of error of $\pm 1 \times 10^{-4}$. The temperature of the apparatus was controlled to within ±0.1 K by a built-in Peltier device. The viscosity and refractive index values were entered into CONTIN algorithm software before measurement as viscosity does affect the size of concentrated solutions via the Stokes−Einstein equation ($R_h = kT/6\pi\eta D_f$) and refractive index values are important for accurate measurement of the scattering vector [$q = (4\pi n_r/\lambda) \sin(\theta/2)$]. Measurement time was varied from 10 to 30 s, and the number of measurements was varied from 25 to 30. Prior to measurements, the cell was rinsed several times with filtered water and then filled with filtered sample solutions. The temperature of the measurements was controlled with an accuracy of ±0.1 K.

2.3. Densimetry. The density (ρ) of the saturated salt solutions at different temperatures was measured with an Anton Paar (Model DMA 4500) vibrating-tube densimeter with a resolution of 5×10^{-2} kg·m^{-3}. The temperature of the apparatus was controlled to within ±0.03 K by a built-in Peltier device that corresponds to uncertainty in density of ±0.0002%. To prevent the uncertainty in the density readings from being affected by the sample viscosity, a number of corrections are needed. Such corrections rely on both the availability of experimental viscosity data over the pressure and temperature ranges considered and the use of properly defined and evaluated damping equations. The deviations between the viscosity corrected and noncorrected density data can climb up from 0.5 to 1% for lower temperatures. In light of the full accuracies of all factors involved in the density readings, an accuracy of $\pm 1 \times 10^{-5}$ g·cm^{-3} for the raw density data is assumed. Reproducibility of the results was confirmed by performing at least three measurements for each sample.

2.4. Ultrasonics. The speed of sound (u) in the salt solutions at varying temperatures was measured at 51600 Hz using a concentration analyzer (Model 87, SCM Laboratory Sonic Composition Monitor) based on the sing-around technique with a single transducer cell, immersed in a water bath with temperature controlled to ±0.01 K. The analyzer was calibrated by measurements of speeds of sound in water as a reference, and the error was estimated to be less than ±0.1 m·s^{-1}. Measurements were carried out in a specially designed sample jar of low volume capacity. Sample jars were provided with an airtight Teflon covering to avoid the sample evaporation during measurements. Not less than three experiments were performed at each temperature to check the reproducibility of the results.

2.5. FT-IR Measurements. FT-IR measurements of saturated aqueous salt solutions were carried out at room temperature using a NICOLET 6700 FT-IR spectrometer. For recording spectra, a cell with BaF_2 windows and a Teflon spacer was used; the optical path length was 0.02 mm. For each spectrum, 132 scans were made with a selected resolution of 4 cm^{-1}.

2.6. NMR Measurements. 1D ^{1}H NMR and 2D DOSY ^{1}H NMR experiments were performed on Bruker Avance 500 MHz NMR spectrometer. Variable-temperature DOSY experiments were acquired using a stimulated echo gradient pulse sequence with a 500 ms diffusion delay, 1200 μs gradient length, 8−16 gradient levels, and 8 scans. Processing DOSY experiments were performed through DOSY software. All chemical shifts were referenced through the water peak of a 0.1 M Na_2SO_4 aqueous solution capillary at 30 °C to 4.8 ppm, and the reference capillary was used externally with respect to saturated aqueous Na_2SO_4 samples. The temperature of the

solutions in a resonance cavity during measurements of concentration dependences of DOSY 2D NMR spectra was fixed with the precision of ±0.1 °C.

3. RESULTS

The solubility of Na_2SO_4 in pure water and in NaCl solutions (5−15 wt %) as a function of temperature is shown in Figure 1.

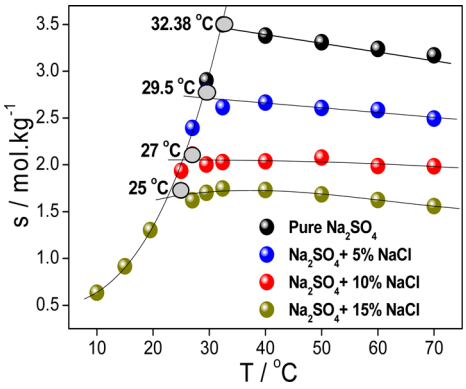

Figure 1. Temperature dependence of Na_2SO_4 solubility in aqueous NaCl solutions.

As established in the literature,[3] the solubility of Na_2SO_4 increases sharply until 32.38 °C and becomes almost constant thereafter. Addition of NaCl decreases both the solubility and solubility transition temperature of Na_2SO_4 while maintaining the basic solubility pattern. It has been observed that the solubility of Na_2SO_4 decreased from 3.5 to 1.72 mol·kg^{-1}, and the solubility transition temperature decreased from 32.38 to 25 °C as the concentration of NaCl in the solution increased to 15 wt %. The temperature dependence (20−70 °C) of Na_2SO_4 solubility in water was probed by examining the saturated solutions through compressibility changes and DLS. Precise measurements of the density and speed of sound (Table S1−S3 in the Supporting Information) allow the determination of solution compressibility (κ_S) by using the Newton−Laplace equation ($\kappa_S = 1/\mu^2\rho$),[13−16] where μ is the speed of sound and ρ is the solution density. Figure 2 shows the variation in κ_S for saturated solutions with or without NaCl. The pattern of κ_S is exactly opposite to that of solubility wherein it decreased with an increase in concentration of Na_2SO_4 until 32.38 °C and increased slightly afterward. With the addition of NaCl (5−15 wt %), although the basic pattern remained the same, the

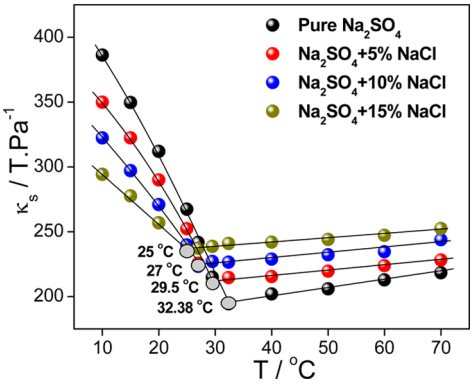

Figure 2. Temperature dependence of κ_S of saturated solutions of Na_2SO_4 containing varying amounts of NaCl.

minimum in κ_S increased from 194 to 235 T·Pa^{-1} with a transition temperature shift from 32.38 to 25 °C, following exactly the solubility trend, albeit in an opposite manner. The DLS measurements of saturated solutions at all of the temperatures showed a bimodal size distribution, that is, a small component corresponding to solvated ions (∼1.5−3 nm) and a large component corresponding to bigger size clusters. A typical plot of the apparent hydrodynamic diameter (D_h) (calculated from the CONTIN method) versus concentration (Figure 3A) shows the growth pattern of clusters in solutions saturated with Na_2SO_4 at different temperatures. As shown in Figure 3B, the cluster size increased for the solutions saturated at increased temperatures and attained a maximum size ($D_h \approx$ 300 nm) for the solution saturated at 32.38 °C, which corresponds to the temperature of the highest solubility. Thereafter, the cluster size started decreasing following the solubility pattern. We also performed the temperature-dependent DLS and κ_S studies for the solutions saturated (i) below the solubility transition temperature and (ii) at the solubility transition temperature. Figure 4A,B shows the CONTIN plots of the hydrodynamic diameter (D_h) versus the normalized intensity of Na_2SO_4−water clusters formed in the saturated solutions at 15 and 32.38 °C, respectively, as a function of temperature. The separate plots of the 15 °C saturated sample at different temperatures showing a smaller solvated ion pair and large cluster are also shown in Figures S2 (Supporting Information). Plots of the apparent hydrodynamic diameter (D_h) versus the intensity of scattered light and κ_S as a function of temperature are compared in Figure 4C,D. For the solution saturated at 15 °C, both the D_h and κ_S decreased from 132 to 107 nm and 347 to 336 T·Pa^{-1}, respectively, with the increase in temperature from 15 to 30 °C, whereas for the solution saturated at 32.38 °C, the D_h and κ_S increased from 300 to 530 nm and 195 to 205 T·Pa^{-1}, respectively, with an increase in temperature from 32.38 to 60 °C, thus showing a similar trend.

The investigated aqueous solutions contain a very high amount of SO_4^{2-} ions having oxygen atoms with a capability of forming hydrogen bonds with the protons of water. Therefore, SO_4^{2-}−H_2O hydrogen bonding interactions in the saturated solutions at different temperatures have been studied by analyzing the vibrational shifts in the characteristic frequency of the OH band of water (νO−H) using FT-IR spectroscopy. The νO−H of water in the saturated Na_2SO_4 aqueous solutions at different temperatures is shown in Figure S3 (Supporting Information). A red shift from 3406 to 3415 cm^{-1} in νO−H has been observed for the Na_2SO_4 saturated solutions in the temperature range of 20−32.38 °C, that is, until the Na_2SO_4 solubility transition temperature, which then starts blue shifting (though very low) for the saturated Na_2SO_4 prepared at still higher temperatures. Further, the FT-IR spectroscopy has been extensively used to study the influence of salts on water structure.[22−30] Curve fitting of the water vibrational spectrum into four deconvoluted bands developed by Walrafen[22] and others[27,28] has been often used for describing the water structure. The deconvoluted FT-IR spectra of pure water and aqueous NaCl (5−15 wt %) solutions saturated with Na_2SO_4 at different temperatures are shown in Figure 5A−E. The prominent bands at around 3250 and 3420 cm^{-1} correspond to the strongly H-bonded patches of water molecules with strongly and weakly H-bonded molecules, respectively. The component bands at 3550 and 3620 cm^{-1} signify coupling of OH asymmetric stretching vibrational modes[24] and the dangling OH stretching modes from three- and two-coordinate

dx.doi.org/10.1021/jp507949h | J. Phys. Chem. B 2014, 118, 12734−12742

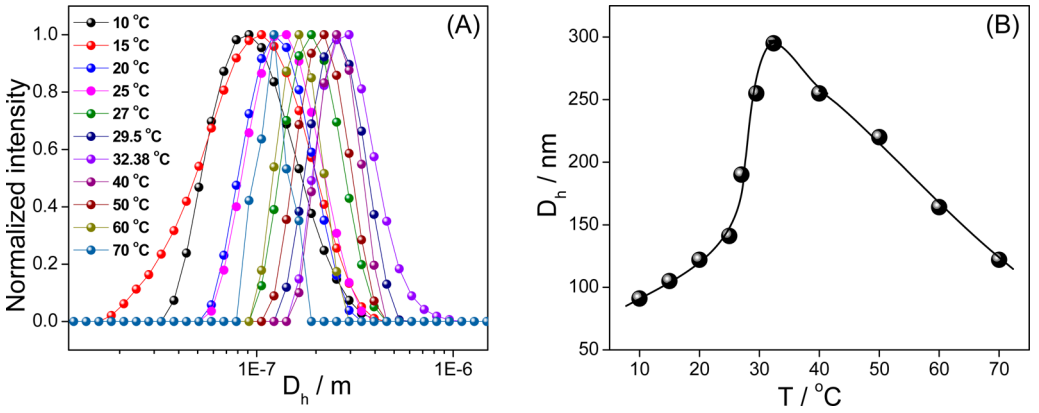

Figure 3. (A) CONTIN plots of the hydrodynamic diameter (D_h) versus the normalized intensity of Na_2SO_4 clusters at different temperatures; (B) cluster size pattern of saturated aqueous Na_2SO_4 at different temperatures.

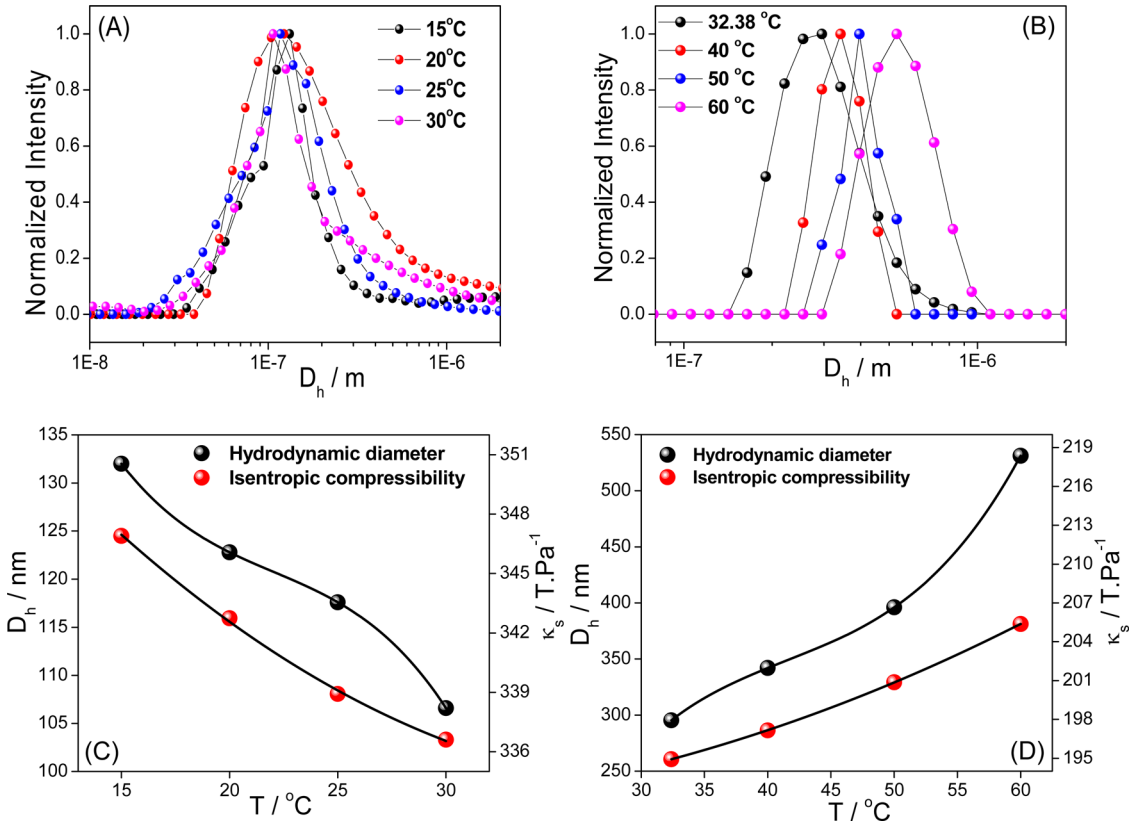

Figure 4. CONTIN plots of the hydrodynamic diameter (D_h) versus the normalized intensity of Na_2SO_4–water clusters in the saturated solutions at 15 (A) and 32.38 °C (B) as a function of temperature. (C,D) Comparison of the variation in D_h and κ_S of the corresponding solutions as a function of temperature.

water molecules, respectively.[29] The deconvoluted spectra for the solutions saturated with Na_2SO_4 and containing varying amounts of NaCl at different temperatures are provided in Figures S4–S6 (Supporting Information). In deconvoluted spectra, A_1, A_2, A_3, and A_4 correspond to the area of bands at 3250, 3420, 3550, and 3620 cm^{-1}, respectively. The band area ratio (BAR) of strongly to weakly H-bonded water molecules $[A_1/(A_2 + A_3 + A_4)]$ provides information about the influence of added salts on the hydrogen bonding network of water and is shown in Figure 5F. The BAR for the solutions saturated with Na_2SO_4 at different temperatures decreases with an increase in concentration, attains a minimum at the solubility transition concentration, and then again increases for the solutions saturated at higher temperatures following the cluster growth pattern, albeit in an opposite manner. The BAR has been found to increase with the addition of NaCl content in the Na_2SO_4 saturated solutions.

The extent of interactions of ion pairs of salts with water molecules in the vicinity can be well understood from the NMR techniques.[31−38] In DOSY NMR , one dimension represents chemical shift data while the second dimension resolves species by their diffusion properties.[39,40] This combination provides a powerful tool for identifying individual species in a system according to their diffusion coefficient. 2D DOSY ^1H NMR spectra of aqueous Na_2SO_4 solutions saturated at different temperatures in the range of 10−70 °C are shown in Figure 6

dx.doi.org/10.1021/jp507949h | J. Phys. Chem. B 2014, 118, 12734−12742

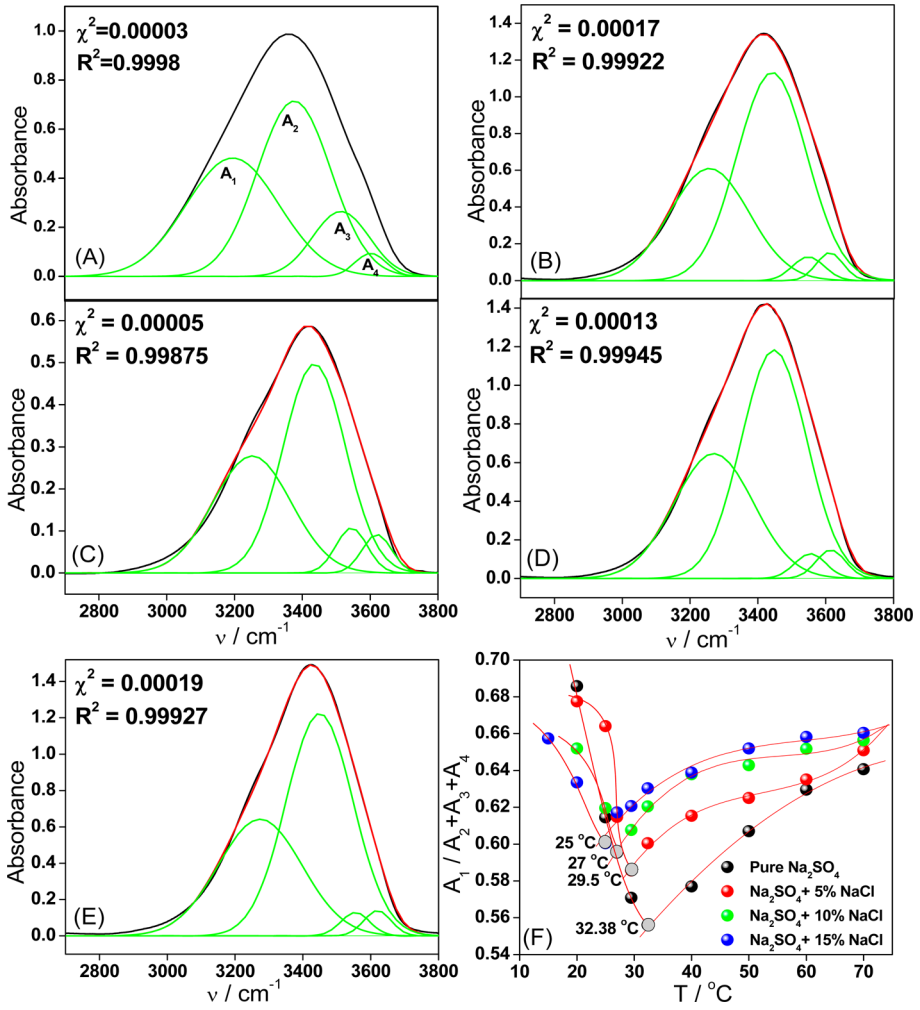

Figure 5. Comparison of deconvoluted FT-IR spectra of water and Na_2SO_4 saturated aqueous solutions containing NaCl at solubility transition temperatures; (A) water, (B) pure aqueous saturated Na_2SO_4, (C) 5 wt % NaCl, (D) 10 wt % NaCl, (E) 15 wt % NaCl, and (F) the BAR of strongly bound (ice like) to weakly H-bonded water molecules (liquid like) of aqueous Na_2SO_4 saturated solutions containing varying amounts of NaCl (5–15 wt %) at different temperatures.

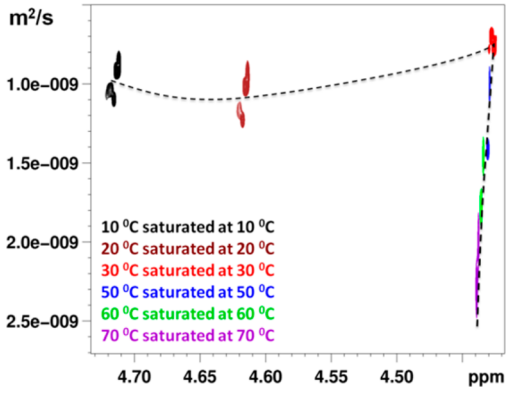

Figure 6. 2D DOSY ^{1}H NMR spectra of aqueous Na_2SO_4 solutions saturated at different temperatures in the range of 10–70 °C (the spectra were recorded for different samples at their corresponding saturation temperature). Dotted lines are just a guide to the eye.

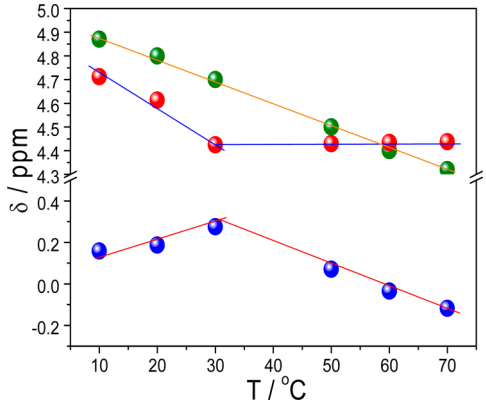

Figure 7. Comparison of ^{1}H NMR chemical shifts (δ) of pure water (green) and aqueous Na_2SO_4 saturated solutions (red) and the contribution of Na_2SO_4 (difference of δ of aqueous Na_2SO_4 saturated solutions and water) (blue) as a function of temperature. Lines are just a guide to the eye.

(spectra were recorded for different samples at their corresponding saturation temperature). The comparison of the ^{1}H chemical shift of pure water and aqueous Na_2SO_4 saturated solutions as a function of temperature is explicitly shown in Figure 7. As compared to pure water, where a continuous upfield shift is observed as a function of temperature,[41] the solutions saturated with Na_2SO_4 showed the upfield shift (though lower than that of water) until 32.38

dx.doi.org/10.1021/jp507949h | J. Phys. Chem. B 2014, 118, 12734–12742

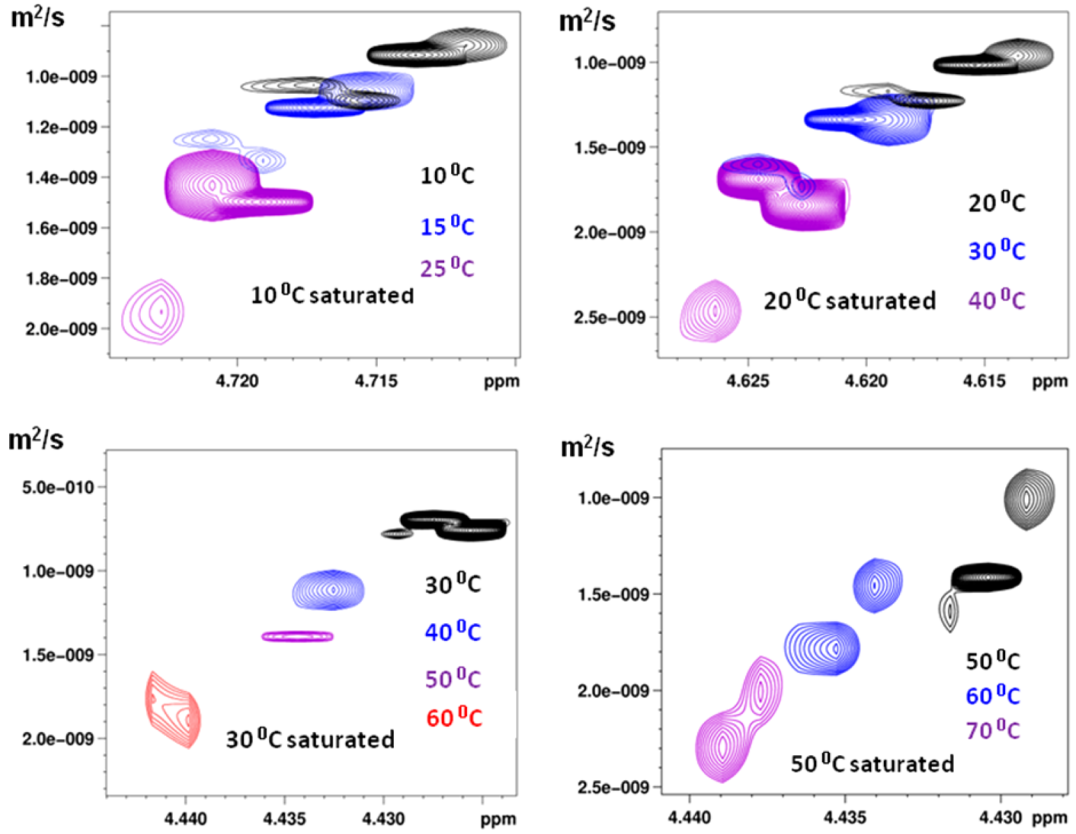

Figure 8. Variable-temperature 2D DOSY ^{1}H NMR spectra of aqueous Na_2SO_4 solutions saturated at 10, 20, 30, and 50 °C.

°C (solubility transition temperature), and thereafter, a small downfield shift was observed until 70 °C.

As indicated by the nature of contours (Figure 6), there exist different types of salt water cluster species with distinct water self-diffusion coefficients for all of the Na_2SO_4 saturated solutions prepared in the investigated temperature range. Nearly constant water self-diffusion coefficients are observed in the temperature range of 10−32.38 °C (1.0×10^{-9} m^2 s^{-1}), whereas at still higher temperatures until 70 °C, it sharply increased to 2.5×10^{-9} m^2 s^{-1}. The temperature variance (an increment of ∼20 °C) of 2D DOSY ^{1}H NMR spectra for the Na_2SO_4 saturated solutions prepared at different temperatures is depicted in Figure 8. An increased water self-diffusion coefficient (an increment of $\sim 1.5 \times 10^{-9}$ m^2 s^{-1}) is observed for all of the Na_2SO_4 saturated solutions with an increase in temperature.

4. DISCUSSION

Comparison of Figures 1 and 2 indicates a good correlation between the temperature-dependent solubility of Na_2SO_4 and κ_S of the solutions saturated with Na_2SO_4. The κ_S of ionic solutions is strongly influenced by the perturbation of the water hydrogen bonding network by the ions and the ionic concentration. The main effect of increasing the ionic concentration is the tendency of the water structure to assume the high density liquid.[42]The κ_S results shows that high-density (less compressible) solutions are formed with an increase in Na_2SO_4 concentration. The lowest value of κ_S is observed at the maximum Na_2SO_4 solubility temperature, indicating the formation of a very rigid solution structure with greatly reduced free volume and hence limits further solubilization of salt. This rigid solution structure is maintained even at higher temperatures, which is in accordance with the nearly constant solubility of Na_2SO_4 after attaining the maximum solubility at the transition temperature. Addition of NaCl reduced the rigidity of the saturated Na_2SO_4 solutions while maintaining the basic pattern of κ_S as a function of temperature, indicating that SO_4^{2-} has a more pronounced effect on perturbation of water H-bonding as compared to the Cl^- ions.[21,43]

DLS (Figure 3A,B) measurements showed the formation of highly stable Na_2SO_4−H_2O clusters in the saturated solutions that tend to grow with the increase in Na_2SO_4 concentration as the temperature increases and attains a maximum D_h at the solubility transition temperature, suggesting that both the concentration and temperature favor the growth of clusters. After attaining the solubility transition temperature, the D_h decreased with the further rise of temperature as a consequence of higher thermal motion between the molecules (Na_2SO_4−H_2O, H_2O−H_2O, or Na_2SO_4−Na_2SO_4). Many factors such as electrostatic interactions among oppositely charged ions, hydrophobic interactions among ions caused by exclusion of ions by water, and bridging of water molecules by anions and/or cations are reported to be responsible for the cluster stability.[44] From an energetics point of view, Peslherbe et al. have reported by using a cluster solvation dielectric model that the large NaI cluster remained stable to ionic dissociation due to very slow convergence of the cluster ion solvation energy with increasing cluster size.[45] In the saturated salt solutions, most of the salt molecules exists in the form of contact ion pairs (CIPs), solvent-shared ion pairs (SSIPs) with the overlapping hydration shells, and solvent-separated ion pairs (2SIPs).[43,45] 2SIP species are reported to be thermodynamically predominant in the larger clusters.,[45] Also, increasing the concentration of salt in solution decreases the number of water molecules

dx.doi.org/10.1021/jp507949h | J. Phys. Chem. B 2014, 118, 12734−12742

available per ion−ion pair due to the alteration of the dipole moment of water solvating the ions and weakening of the water hydrogen bonding network.[46] From a temperature point of view, the O−H stretch lifetimes of salt solutions decrease with an increase in temperature due to an increase in anharmonic interaction with the increasing thermal occupation of accepting modes.[47] Further, when the hydration shell of an anion is shared by a cation forming a $Y^+OH\cdots X^-$ structure (in the present case, $Y = Na^+$, and $X = SO_4^{2-}$), the cation modifies the properties of the associated anion−water H-bond.[48] The effect becomes more pronounced as the charge on the cation increases, leading to stronger H-bonds and thereby anchoring the water molecules strongly in Na_2SO_4−water clusters. In the Na_2SO_4−water clusters "at the solubility maximum", the dipoles resulting from this local alignment of solvated water grow large enough to slow down the equilibrium of bulk and solvated water, thus minimizing the hydration of additional amounts of Na_2SO_4 with the further rise in temperature. A view on the correlation of cluster size and the solubility behavior of Na_2SO_4 is further obtained by analyzing the temperature dependence of D_h or κ_S of 15 °C (well below the solubility transition temperature) and 32.38 °C (at the solubility transition temperature) saturated solutions of Na_2SO_4 (Figure 4). The decrease in D_h and κ_S seen for the 15 °C saturated solution until it is heated to the solubility transition temperature indicates reduction of free volume and release of water molecules from the cluster, which possibly are being utilized for the dissolution of more quantity of salt, and hence, an increase in the solubility of Na_2SO_4 is observed in this temperature range. On the other hand, the increase in D_h and κ_S observed for the 32.38 °C saturated solution of Na_2SO_4 upon further heating indicates enhanced solution compressibility as a consequence of loosening of H-bonds by thermal assistance and/or accommodation of more water molecules in the cluster. Therefore, nonavailability of free water molecules restricts dissolution of extra salt and leads to a nearly constant solubility of Na_2SO_4 after the transition temperature. We further verified these results by measuring the variation in D_h of a 50 °C saturated Na_2SO_4 solution at 60 and 70 °C and found the similar trend (Figure S7, Supporting Information). These results find support from the statement "cooperativity in ion hydration" for the salts having both strongly hydrated cations and anions that interlock the hydrogen bonding network in multiple directions in a cluster.[49] Because the rise in temperature always affects the thermal motion of molecules, in a saturated Na_2SO_4−H_2O cluster, the thermal motion due to an increase in temperature weakens the hydrogen bonding of water around the clusters, causing expansion in size, but the interlocking effect of Na_2SO_4 at the saturated concentration does not allow the water molecules to leave the clusters.

The extent of water hydrogen bonding distortion in the Na_2SO_4 saturated solutions containing varying amounts of NaCl is evident from FT-IR results (Figure 5). The electric field of the Na^+ ions polarizes the O−H···O and O−H···SO_4^{2-} H-bonds of water molecules adjacent to it. The strength of the H-bonds increases with increasing polarization and alters the O−H stretch vibration of a H_2O molecule solvating the anion.[21] The small BAR value for Na_2SO_4−water saturated solutions (which further decreased from 0.67 to 0.55 at the solubility transition temperature, Figure 5F) compared to that of pure water (1.07) indicated perturbation of the water H-bonding network by Na^+ and SO_4^{2-} ions to a marked extent, in line with the compressibility data. In a recent report, Stirnemann et al. have concluded from simulation and analytical modeling of concentrated aqueous solutions of Na_2SO_4 and $NaClO_4$ that at high concentration, the effect on water acceleration and retardation is independent of the ionic nature of the salt and is governed by a viscosity factor.[43] We further verified their statement by measuring the BAR value of 3.5 m NaCl (0.58) and found it near to that of 3.5 m Na_2SO_4 (0.55). The increased BAR value after the solubility transition temperature indicated strengthening of water H-bonding as a consequence of decreased ion−water interaction and enhanced hydrophobic hydration. Therefore, it can be inferred that after the solubility transition temperature, salt tends to become anhydrous and water tends to regain its original structure. The changes in ^1H NMR also provided valuable clues on the nature of the interactions (Figures 6 and 7). A downfield shift observed until the solubility transition temperature in the differential ^1H chemical shift of water and aqueous Na_2SO_4 saturated solutions shows deshielding of the hydrogen nucleus under the influence of a more electropositive Na^+ cation and is indicative of strong $SO_4^{2-}\cdots H-O-H$ bonds, whereas upfield shift observed after the solubility transition temperature indicates weakening of $SO_4^{2-}\cdots H-O-H$ bonds, complementing the FT-IR results. H-bonding protons have especially pronounced dependence of resonance frequency on the sample temperature. An increase in temperature results in weakening of the H-bonds and therefore reduction in the electron-withdrawing effect of the H-bond acceptor on the proton. As a result, the proton becomes more shielded, and its chemical shift decreases. 2D DOSY ^1H NMR spectra provides additional information on individual species in a system according to their diffusion coefficient (Figure 6). The nature of contours indicates existence of different types of salt water cluster species with distinct water self-diffusion coefficients (though at a very small time scale) for all of the Na_2SO_4 saturated solutions. A nearly constant water self-diffusion coefficient observed in the temperature range of 10−32.38 °C ($\sim 1.0 \times 10^{-9}$ m^2s^{-1}) is due to the opposing effect of ions/ionic concentration and temperature on the dynamics of the water molecules. The hydration of the ions or increase in concentration of the ions, particularly of a structure-making salt, such as Na_2SO_4, causes a decrease in the diffusion constant of water molecules, whereas the disruption of the H-bond network with thermal assistance causes an increase in the diffusion constant of the water molecules.[50] Overall, herein, it seems that a balance is maintained between these opposing effects until the solubility transition temperature is achieved. At higher temperatures, that is, >32.38 °C until 70 °C, a sharp increase in self-diffusion of water is due to the abrupt dehydration of Na_2SO_4, and self-diffusion of water is solely driven by a temperature factor wherein water molecules become more mobile because of highly reduced ion−water interactions and weakened H-bonds. This is in accordance with the FT-IR results wherein weakening of ion−water interactions is observed and water starts regaining its native structure, thereby not participating in further dissolution Na_2SO_4 after the solubility transition temperature. The significant increase of the diffusion coefficient found in the temperature variance of 2D DOSY ^1H NMR spectra for the Na_2SO_4 saturated solutions prepared at different temperatures (Figure 8) shows the dominance of the temperature factor over Na_2SO_4−water interactions for all of the saturated solutions. However, there is an indication of the merging of various cluster species for the saturated solutions nearing the solubility transition temperature

dx.doi.org/10.1021/jp507949h | J. Phys. Chem. B 2014, 118, 12734−12742

resulting in the growth of clusters, whereas for the saturated solutions above the solubility transition temperature, different cluster species, namely, Na_2SO_4–water and water–water, start to emerge probably because of the dehydration of Na_2SO_4 and water not participating in further dissolution of Na_2SO_4.

5. CONCLUSION

The temperature-dependent solubility transition of Na_2SO_4 in water is correlated with the growth and stability of Na_2SO_4–water clusters. The nature of the clusters and their stabilities were probed by a combination of measurements including DLS, compressibility, and FT-IR/2D DOSY ^{1}H NMR spectroscopy. Expansion in the cluster size until the solubility transition temperature is attained indicates increased solvation of Na_2SO_4 in the clusters. The shrinking of cluster size as a function of temperature for a particular Na_2SO_4 saturated solution well below the solubility transition temperature shows that the water released is available for the solubilization of an additional amount of Na_2SO_4. After the solubility transition temperature, a nearly constant solubility of Na_2SO_4 as a function of temperature is the consequence of (i) weakened Na_2SO_4–water interactions in the clusters, (ii) a highly perturbed water hydrogen bonding network with reduced capacity to solvate ions–ion pairs, and (iii) high rigidity of an aqueous Na_2SO_4 saturated solution preventing the penetration of Na_2SO_4 further into the solution. The addition of NaCl decreased the solubility transition temperatures of Na_2SO_4 as a consequence of decreased Na_2SO_4–water interactions because of competing effects of Cl^{1-} and SO_4^{2-} ions in the solution wherein the latter has more pronounced effect on the water structure. The studies are important in practical processes such as the separation of Na_2SO_4 from natural brine systems and industrial effluents containing these salts. Unravelling the phenomenon at a more fundamental level using simulation techniques would be a logical extension of the above work.

■ ASSOCIATED CONTENT

Supporting Information

Annexure 1 showing gravimetric calculation of the Na_2SO_4 concentration in aqueous solution, Figure S1 showing the temperature-dependent solubility of alkali metal sulfates, Figures S2 showing CONTIN plots of 15 °C saturated Na_2SO_4 at different temperature, Figures S3–S6 showing deconvoluted FT-IR spectra of pure aqueous saturated Na_2SO_4 and at a Na_2SO_4 + NaCl mixture, Figure S7 showing CONTIN plots of 50 °C saturated Na_2SO_4 at different temperature, and Tables S1–S3 showing density and speed of sound values of aqueous saturated Na_2SO_4 solutions are provided. This material is available free of charge via the Internet at http://pubs.acs.org.

■ AUTHOR INFORMATION

Corresponding Author

*E-mail: mailme_arvind@yahoo.com or arvind@csmcri.org. Phone: +91-278-2567039. Fax: +91-278-2567562.

Notes

The authors declare no competing financial interest.

■ ACKNOWLEDGMENTS

This work is carried out under a CSIR Supra Institutional Project CSC-0203. The authors thank the Analytical Discipline and Centralized Instrumental Facility of the Institute for Technical Analysis. The authors are also thankful to Dr. Bishwajit Ganguly and Rabindranath Lo for the helpful discussions.

■ REFERENCES

(1) von Plessen, H. Sodium Sulfates. *Ullmann's Encyclopedia of Industrial Chemistry*; Verlag Chemie: Weinheim, Germany, 1993.
(2) Rosenblatt, D.; Marks, S. B.; Pigford, R. L. Kinetics of Phase Transitions in the System Sodium Sulfate–Water. *Ind. Eng. Chem. Fundam.* **1984**, *23*, 143–147.
(3) Linke, W. F. *Solubilities of Inorganic and Metal Organic Compounds*; American Chemical Society: Washington, DC, 1965.
(4) Georgalis, Y.; Kierzek, A. M.; Saenger, W. Cluster Formation in Aqueous Electrolyte Solutions Observed by Dynamic Light Scattering. *J. Phys. Chem. B* **2000**, *104*, 3405–3406.
(5) Bharmoria, P.; Gupta, H.; Mohandas, V. P.; Ghosh, P. K.; Kumar, A. Temperature Invariance of NaCl Solubility in Water: Inferences from Salt–Water Cluster Behavior of NaCl, KCl, and NH_4Cl. *J. Phys. Chem. B* **2012**, *116*, 11712–11719.
(6) Bernal, J. D.; Fowler, R. H. A Theory of Water and Ionic Solution, with Particular Reference to Hydrogen and Hydroxyl Ions. *J. Chem. Phys.* **1933**, *1*, 515–548.
(7) Onsager, L.; Fuoss, R. M. Irreversible Processes in Electrolytes. Diffusion, Conductance and Viscous Flow in Arbitrary Mixtures of Strong Electrolytes. *J. Phys. Chem.* **1932**, *36*, 2689–2778.
(8) Markus, Y. Ionic Radii in Aqueous Solutions. *Chem. Rev.* **1988**, *88*, 1475–1498.
(9) Jenkins, H. D. W.; Markus, Y. Viscosity *B*-Coefficients of Ions in Solution. *Chem. Rev.* **1995**, *95*, 2695–2724.
(10) Marcus, Y.; Hefter, G. Ion Pairing. *Chem. Rev.* **2006**, *106*, 4585–4621.
(11) Ohtali, H.; Randnai, T. Structure and Dynamics of Hydrated Ions. *Chem. Rev.* **1993**, *93*, 1157–1204.
(12) Robinson, R. A.; Stokes, R. H. *Electrolyte Solutions: The Measurement and Interpretation of Conductance, Chemical Potential and Diffusion in Solutions of Simple Electrolytes*; Academic Press: New York, 1959.
(13) Passynski, A. Compressibility and Solvation of Solutions of Electrolytes. *Acta Physicochim.* **1938**, *8*, 385–418.
(14) Mathieson, J. G.; Conway, B. E. Partial Molal Compressibilities of Salts in Aqueous Solution and Assignment of Ionic Contributions. *J. Solution Chem.* **1974**, *3*, 455–477.
(15) Gucker, F. T.; Stubley, D.; Hill, D. J. The Isentropic Compressibilities of Aqueous Solutions of Some Alkali Halides at 298.15 K. *J. Chem. Thermodyn.* **1975**, *7*, 865–873.
(16) Onori, G. *Acoust. Lett.* **1990**, *14*, 7–15.
(17) Kropman, M. F.; Bakker, H. J. Dynamics of Water Molecules in Aqueous Solvation Shells. *Science* **2001**, *291*, 2118–2120.
(18) Max, J. J.; Chapados, C. IR Spectroscopy of Aqueous Alkali Halide Solutions: Pure Salt-Solvated Water Spectra and Hydration Numbers. *J. Chem. Phys.* **2001**, *115*, 2664–2675.
(19) Cerreta, M. K.; Berglund, K. A. J. The Structure of Aqueous Solutions of Some Dihydrogen Orthophosphates by Laser Raman Spectroscopy. *Cryst. Growth* **1987**, *84*, 577–587.
(20) Dillon, S. R.; Dougherty, R. C. NMR Evidence of Weak Continuous Transitions in Water and Aqueous Electrolyte Solutions. *J. Phys. Chem. A* **2003**, *107*, 10217–10224.
(21) Bakker, H. J. Structural Dynamics of Aqueous Salt Solutions. *Chem. Rev.* **2008**, *108*, 1456–1473.
(22) Walrafen, G. E. In *Water, A Comprehensive Treatise*; Franks, F., Ed.; Plenum: New York, 1972; Vol. *I*, Chapter 5.
(23) Narten, A. H.; Levy, H. A. In *Water, A Comprehensive Treatise*; Franks, F., Ed.; Plenum; New York, 1972; Vol. *I*, Chapter 8.
(24) Du, Q.; Superfine, R.; Freysz, E.; Shen, Y. R. Vibrational Spectroscopy of Water at the Vapor/Water Interface. *Phys. Rev. Lett.* **1993**, *70*, 2313–2316.
(25) Kusalik, P. G.; Svishchev, I. M. The Spatial Structure in Liquid Water. *Science* **1994**, *265*, 1219–21.
(26) Tanaka, H. Cavity Distribution in Liquid Water and Hydrophobic Hydration. *Chem. Phys. Lett.* **1998**, *282*, 133–138.

(27) Green, J. L.; Lacey, A. R.; Sceats, M. G. Spectroscopic Evidence for Spatial Correlations of Hydrogen Bonds in Liquid Water. *J. Phys. Chem.* **1986**, *90*, 3958−3964.
(28) Hare, D. E.; Sorensen, C. M. Interoscillator Coupling Effects on the O−H Stretching Band of Liquid Water. *J. Chem. Phys.* **1992**, *96*, 13−23.
(29) Rowland, B.; Fisher, M.; Delvin, J. P. Probing Icy Surfaces with the Dangling-OH-Mode Absorption: Large Ice Clusters and Microporous Amorphous Ice. *J. Chem. Phys.* **1991**, *95*, 1378−85.
(30) Gopalakrishnan, S.; Jungwirth, P.; Tobias, D. J.; Allen, H. C. Air−Liquid Interfaces of Aqueous Solutions Containing Ammonium and Sulfate: Spectroscopic and Molecular Dynamics Studies. *J. Phys. Chem. B* **2005**, *109*, 8861−8872.
(31) Reuben, J. Hydrogen-Bonding Effects on Oxygen-17 Chemical Shifts. *J. Am. Chem. Soc.* **1969**, *91*, 5725−5729.
(32) Svishchev, I. M.; Kusalik, P. G. Proton Chemical Shift of Water in the Liquid State: Computer Simulation Results. *J. Am. Chem. Soc.* **1993**, *115*, 8270−8274.
(33) Li, R.; Jiang, Z.; Shi, S.; Yang, H. Raman Spectra and ^{17}O NMR Study Effects of $CaCl_2$ and $MgCl_2$ on Water Structure. *J. Mol. Str.* **2003**, *645*, 69−75.
(34) Irish, D. E. In *Ionic Interactions*; Petruchi, S., Ed.; Academic Press: New York, 1971; Vol. *II*, p 187.
(35) Bloor, E. G.; Kidd, R. G. Solvation of Sodium Ions Studied by ^{23}Na Nuclear Magnetic Resonance. *Can. J. Chem.* **1968**, *46*, 3425−3430.
(36) Erlich, R. H.; Popov, A. I. Spectroscopic Studies of Ionic Solvation. X. Study of the Solvation of Sodium Ions in Nonaqueous Solvents by Sodium-23 Nuclear Magnetic Resonance. *J. Am. Chem. Soc.* **1971**, *93*, 5620−5623.
(37) Miller, A. G.; Franz, J. A.; Macklin, J. W. Chlorine-35 Nuclear Magnetic Resonance Study of Aqueous Sodium Perchlorate Association. *J. Phys. Chem.* **1985**, *89*, 1190−1193.
(38) Weeding, T. L.; Veeman, W. S. Characterisation of the Structure of Inorganic Chloride Salts with Chloride Solid State NMR. *J. Chem. Soc., Chem. Commun.* **1989**, 945−946.
(39) Morris, K. F.; Johnson, C. S., Jr. Diffusion-Ordered Two-Dimensional Nuclear Magnetic Resonance Spectroscopy. *J. Am. Chem. Soc.* **1992**, *114*, 3139−3141.
(40) Li, D.; Keresztes, I.; Hopson, R.; Williard, P. G. Characterization of Reactive Intermediates by Multinuclear Diffusion-Ordered NMR Spectroscopy (DOSY). *Acc. Chem. Res.* **2009**, *42*, 270−280.
(41) Hoffman, R. E. Standardization of Chemical Shifts of TMS and Solvent Signals in NMR Solvents. *Magn. Reson. Chem.* **2006**, *44*, 606−616.
(42) Gallo, P.; Corradinib, D.; Roverea, M. Ion Hydration and Structural Properties of Water in Aqueous Solutions at Normal and Supercooled Conditions: A Test of the Structure Making and Breaking Concept. *Phys. Chem. Chem. Phys.* **2011**, *13*, 19814−19822.
(43) Stirnemann, G.; Wernersson, E.; Jungwirth, P.; Laage, D. Mechanisms of Acceleration and Retardation of Water Dynamics by Ions. *J. Am. Chem. Soc.* **2013**, *135*, 11824−11831.
(44) Degréve, L.; da Silva, F. L. Structure of Concentrated Aqueous NaCl Solution: A Monte Carlo Study. *J. Chem. Phys.* **1999**, *110*, 3070−3079.
(45) Peslherbe, G. H.; Ladanyi, B. M.; Hynes, J. T. Free Energetics of NaI Contact and Solvent-Separated Ion Pairs in Water Clusters. *J. Phys. Chem. A* **2000**, *104*, 4533−4548.
(46) Wachter, W.; Kunz, W.; Buchner, R.; Hefter, G. Is There an Anionic Hofmeister Effect on Water Dynamics? Dielectric Spectroscopy of Aqueous Solutions of NaBr, NaI, $NaNO_3$, $NaClO_4$, and NaSCN. *J. Phys. Chem. A* **2005**, *109*, 8675−8683.
(47) Abraham, N.; Joshua, J. Vibrational Relaxation of a Molecule in a Dense Medium. *Mol. Phys.* **1973**, *25*, 713−734.
(48) Heisler, I. A.; Mazur, K.; Meech, S. R. Low-Frequency Modes of Aqueous Alkali Halide Solutions: An Ultrafast Optical Kerr Effect Study. *J. Phys. Chem. B* **2011**, *115*, 1863−1873.
(49) Tielrooij, K. J.; Garcia-Araez, N.; Bonn, M.; Bakker, H. J. Cooperativity in Ion Hydration. *Science* **2010**, *328*, 1006−1009.
(50) Kim, J. S.; Wu, Z.; Morrow, A. R.; Yethiraj, A. Self-Diffusion and Viscosity in Electrolyte Solutions. *J. Phys. Chem. B* **2012**, *116*, 12007−12013.